Underground Design Methods 2015 – Y Potvin (ed.)

doi:10.36487/ACG_rep/1511_33_Veenstra

A methodology for predicting dilution of cemented paste backfill

RL Veenstra *Glencore Mount Isa Mines, Australia*

Abstract

This paper presents results from a numerical modelling exercise that looks at predicting the amount of backfill dilution expected from vertically exposed cemented paste backfill (CPB). The paper initially presents the process by which model input parameters were determined from laboratory testing and then shows how the model and laboratory results compare. The paper then presents the methodology for determining when the vertically exposed backfill mass fails and for calculating the amount of backfill dilution from this failure. A series of models were run for simple rectangular stopes for easy comparison to existing analytical exposure models. Finally, a case study was conducted by comparing the results of the methodology to cavity monitoring survey (CMS) data from an underground stope.

1 Introduction

The backfilling of underground mine voids, or stopes, is a common practice at many mining operations worldwide as it allows for maximal ore extraction and provides regional ground support. Many types of backfill exist, but CPB has gained in popularity due to its delivery speed, its versatility, and its engineered strength.

In order to achieve maximal ore recovery it is usually necessary for the placed backfill to be exposed, either vertically or horizontally, when adjacent stopes are blasted and mucked. Due to this exposure, the backfill needs to be strong enough to prevent it from failing into the recently voided stope. If not, the backfill will fail and cause backfill dilution into the stope.

This paper presents the results of a numerical modelling exercise that looks to correlate backfill strength, vertical exposure size, and expected dilution. The modelling was completed using Itasca's FLAC3D numerical modelling software (Itasca Consulting Group, Inc. 2015).

2 Input parameters

This section deals with how the input parameters for the modelling were derived from laboratory testing. The laboratory testing consisted of both unconfined compressive strength (UCS) testing as well as tensile (or Brazilian) disc testing. The tensile disc testing was conducted to give an approximate idea of how the tensile strength of the CPB related to its UCS.

2.1 Laboratory tests

Figure 1 contains the axial stress–strain curves measured from the UCS testing program. Note that this graph combines results from three different cement contents (2, 4 and 6% by solids mass) at different curing ages. These results were combined, as the purpose of this exercise was to examine paste strength variation, and not what cement percentage or curing age that would be required (although this could be determined later). Note that the lower strength UCS tests show much more ductile behaviour then the higher strength UCS tests.

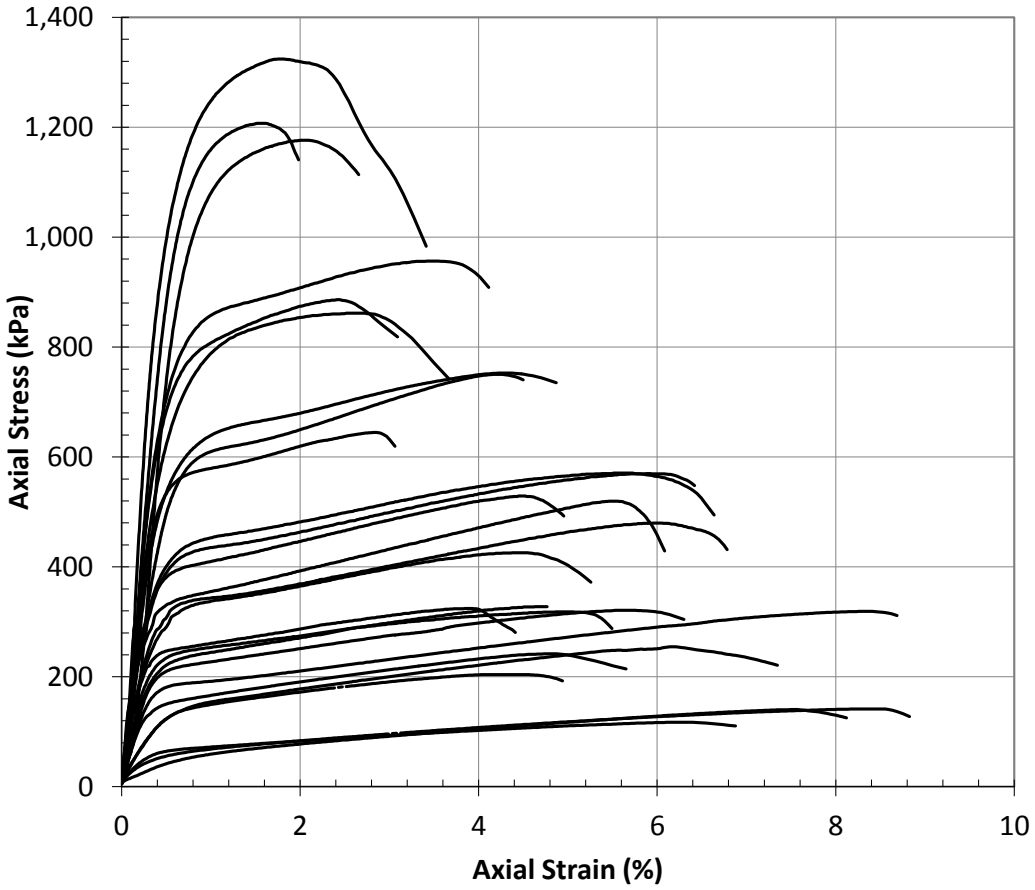

Figure 1 Unconfined compressive strength testing results

Figure 2 correlates the UCS test results with the tensile disc testing results. Ignoring the lower two outliers, this correlation shows that the tensile strength of the CPB is typically 20% of the UCS. This is similar to the UCS-tension correlation shown in Hughes (2014).

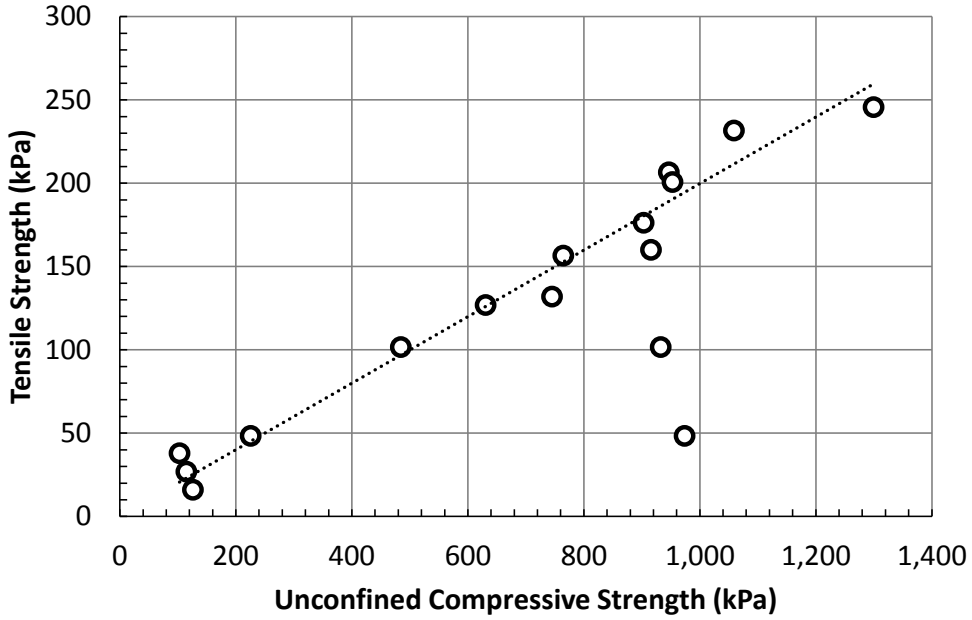

Figure 2 Comparing unconfined compressive strength to tensile disc results

2.2 Model calibration to laboratory tests

All of the models were conducted using FLAC3D's strain-softening constitutive model. Inputs for this model include density, deformation parameters (bulk and shear moduli), and strength parameters (cohesion, tension and friction angle).

Initial estimates of these parameters were determined either directly from the laboratory testing results or indirectly from the results and other assumed material properties. For example, density was determined directly from the laboratory results, but the deformation parameters were calculated using the elastic modulus, as determined from the UCS testing (Figure 3), and an assumed Poisson's ratio of 0.25 was adopted. Likewise, the material cohesion was calculated using the UCS value and a friction angle of 30 degrees. Tension was calculated using the relationship determined in Figure 2.

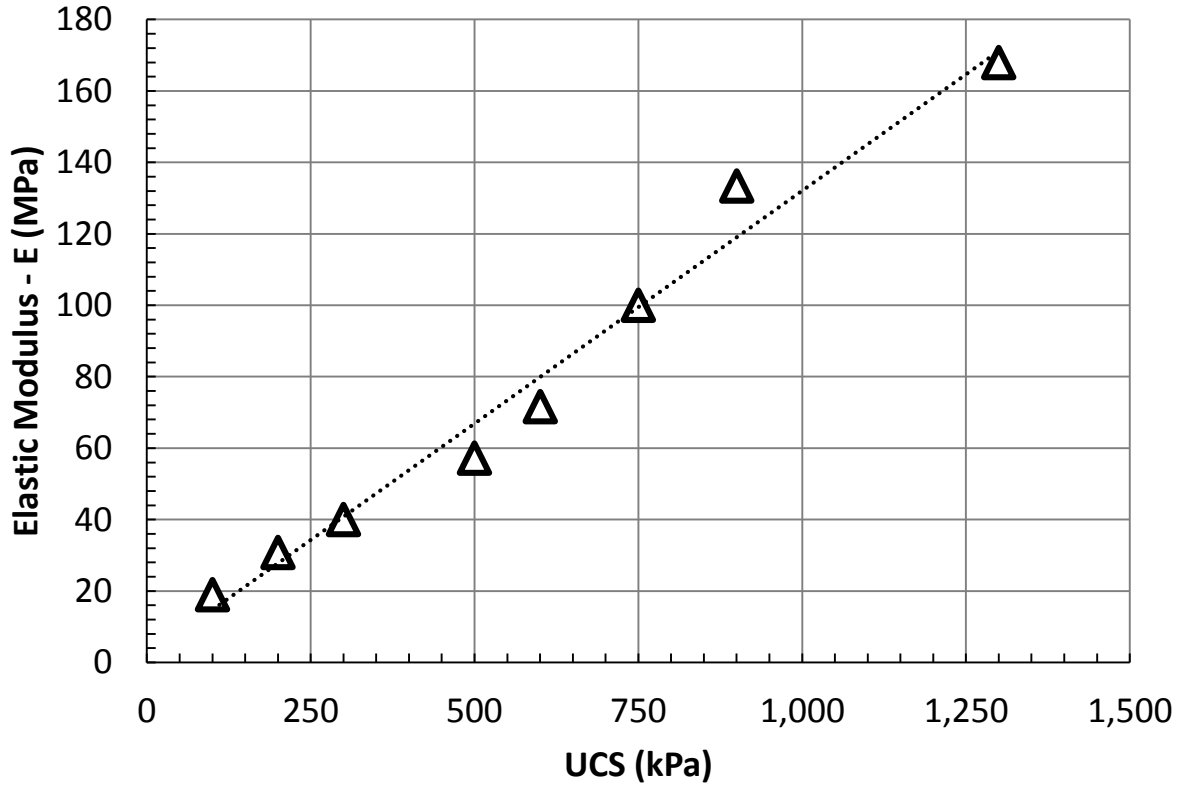

Figure 3 Comparing unconfined compressive strength to elastic modulus

The use of a strain-softening model allows for the post-peak behaviour of the material to be captured. This is particularly important as CPB can exhibit ductile to brittle behaviour (depending on cement percentage and curing age). FLAC3D's strain-softening model does this by reducing the strength of the material to zero over a given plastic strain, called the critical strain. Each UCS models' post-peak behaviour was determined by an iterative process of modifying the model's critical strains and comparing the results to the laboratory data.

An example of this process is shown in Figure 4. The grey zones in the modelled cylinder have the inputted initial cohesion of the material. The model initially demonstrates strain hardening corresponding to an increase in cohesion (white zones). After a zone reaches a maximum cohesion value, its cohesion decreases to zero (black zones) and indicates an area where shear failure is likely.

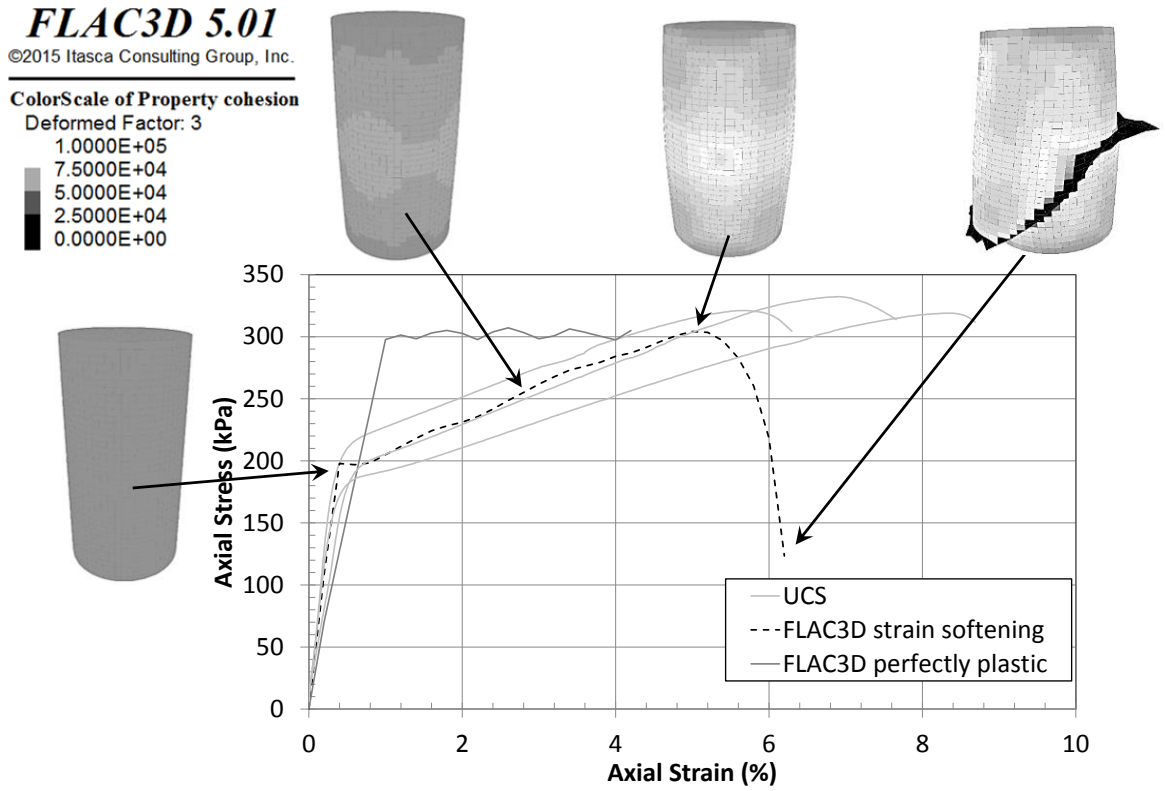

Figure 4 Calibrated 300 kPa UCS model (including perfectly plastic model curve)

2.3 Summary of input parameters

Figure 5 compares the initial UCS results from Figure 1 (black lines) to the calibrated modelled results (dashed grey lines). This comparison of the laboratory curves and the model curves results in similar trends being observed.

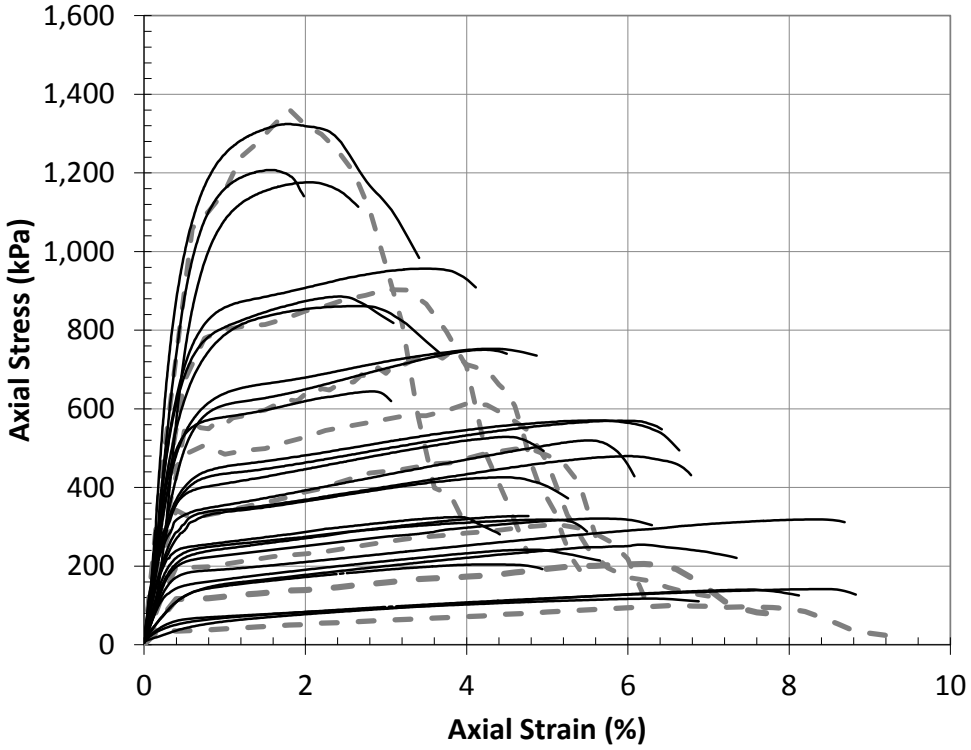

Figure 5 Comparison of laboratory UCS results and calibrated model curves

3 Modelling results

This section presents how the modelling was conducted. Modelling results obtained from two different model geometries are then analysed and discussed.

3.1 Vertical stability classification

Vertical stope stability can generally be classified into three categories: negligible, surficial/transitional, and deep, and are shown schematically in Figure 6. These classifications generally correlate, in the author's experience, to less than 5% backfill dilution, 5 to 10% backfill dilution, and more than 10% backfill dilution respectively. The first two categories are generally due to an outside interaction with the paste (e.g. relaxation within the fill mass due to the rock surface being removed or poor blasting practices (van Gool 2007). The third (and possibly the second) category is due to a failure of the fill mass itself.

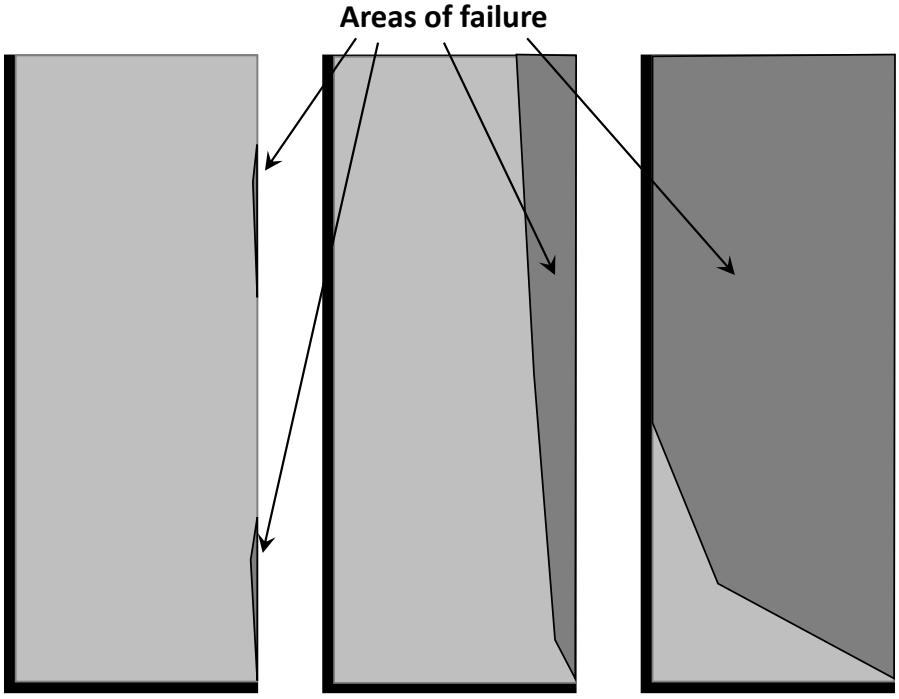

Figure 6 Classification of vertical stope stability: (a) negligible; (b) surficial/transitional; and (c) deep

3.2 Modelling methodology

In order to more accurately determine the stresses within the stope, the paste was placed in the stope in a series of stages within a rock mould. This was done to replicate the actual filling of the stopes and to account for the stress arching within the stopes. Not accounting for this arching can cause the initial stresses, particularly at the bottom of high and complex geometry stopes, to be overestimated.

Once filled, the paste was exposed by nulling the appropriate section of rock. Once exposed, the unbalanced forces, displacements and velocities of the paste, were monitored. Figure 7 illustrates the typical stable and unstable behaviour. In unstable behaviour, parts of the stope will continually displace and exhibit accelerations. In stable behaviour the displacements will plateau and the velocities will reduce to zero.

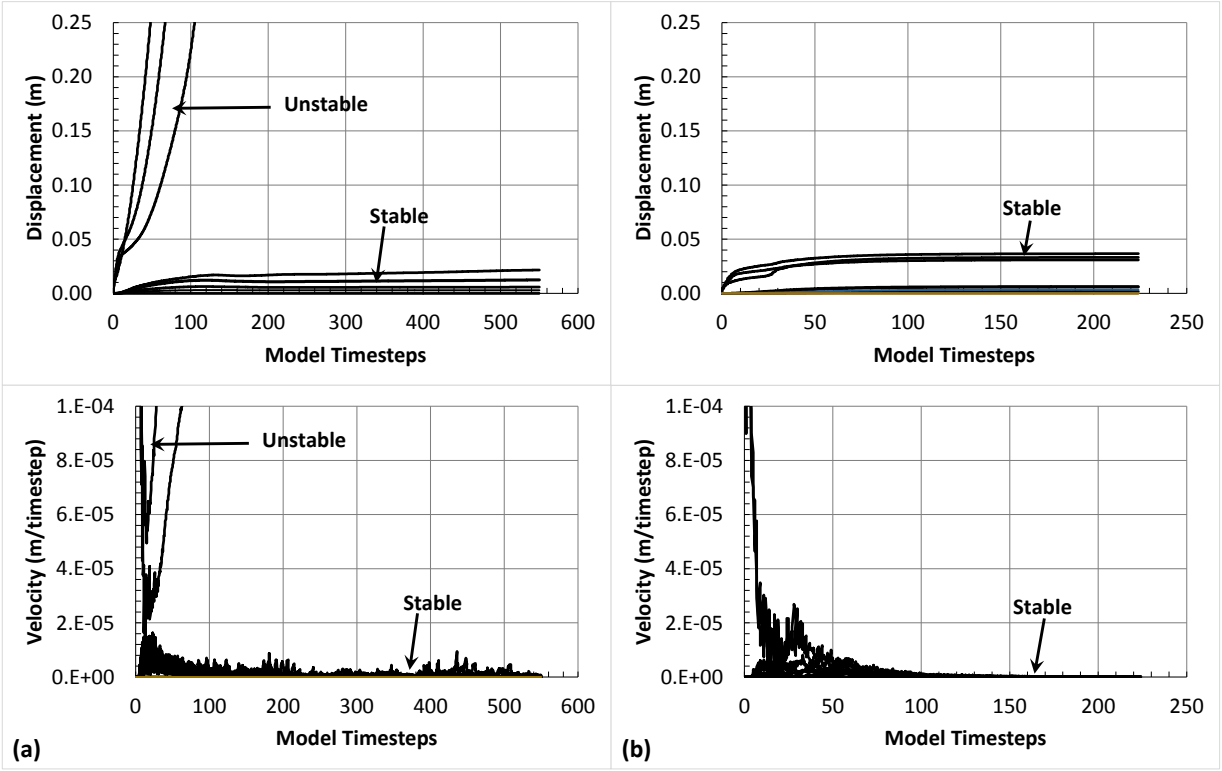

Figure 7 Displacement and velocity monitoring for (a) unstable and (b) stable exposures

Note that the unstable curves in Figure 7(a) are from monitoring points immediately next to an exposure surface. The stable curves in Figure 7(a) are for monitoring points located further into the fill mass (hence stable) whereas the stable curves in Figure 7(b) indicate that the entire fill mass is stable. The velocity curves in the unstable exposure do reduce, but are more unstable when compared to the stable exposure model (Figure 7(b)).

However, the above methodology only indicates that the stope has started to yield but does not give an indication of the amount of dilution that can be expected. This can be estimated by examining the post-peak behaviour of the CPB. Figure 8 shows several model plots of a failed exposure.

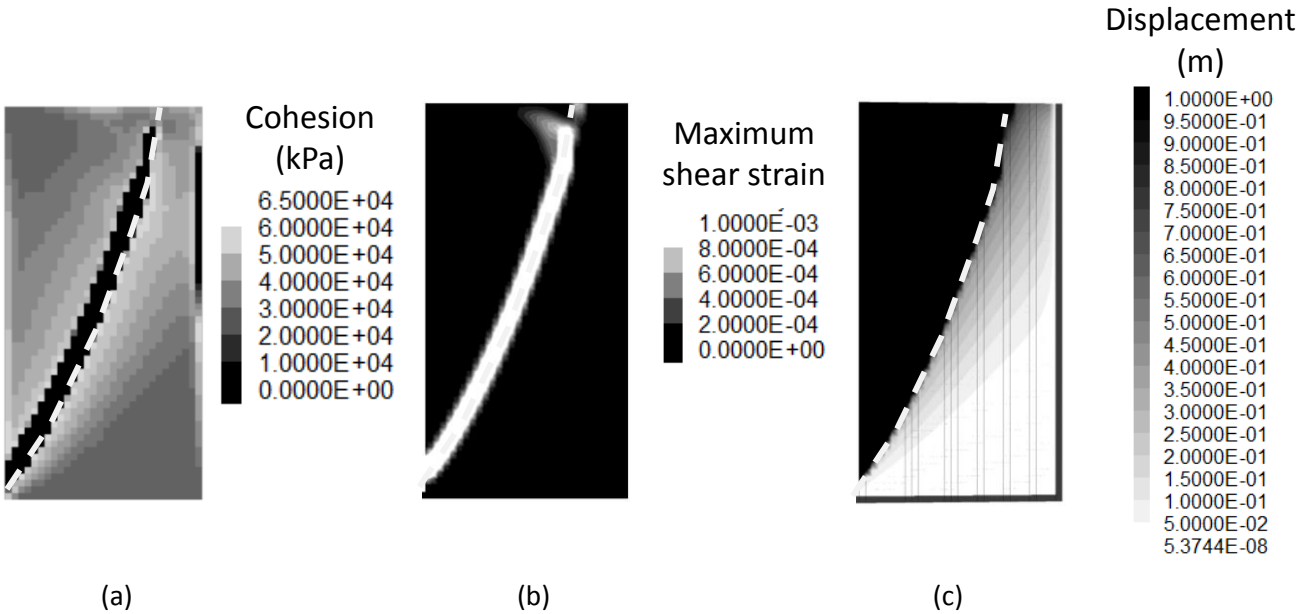

Figure 8 Model plots showing (a) cohesion; (b) maximum shear strain rate; and (c) displacement

Figure 8(a) shows a band of zero-cohesion zones indicating an area where shear failure is possible. This is further collaborated by the white shear rate band shown in Figure 8(b). The displacement plot in Figure 8(c) shows an area of high displacement (delineated by the dashed line). This plot shows the development of a 'stable' failure surface, meaning that the part of the stope above the dashed line continues to displace along the shear band while the section below the shear band exhibits minimal displacement. Part of the model algorithm monitors the size of yielded volume to determine when this volume stabilises. An example is shown in Figure 9.

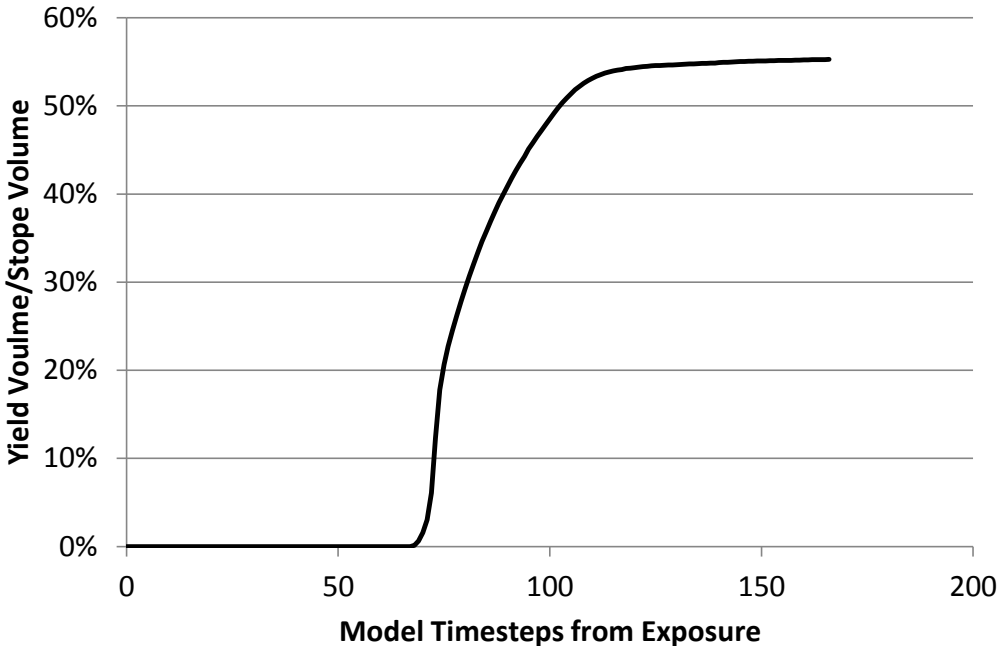

Figure 9 Yield volume stabilisation with time-step

As the above methodology is controlled by the critical strain it is important to examine scaling the calibrated UCS model critical strain values (obtained at a small model zone size) to the exposure model zone size (50 cm in the case of all models presented in this paper). In general, scaling critical strain from a smaller zone size to a larger size makes the response more brittle while the opposite is true for a decrease in zone size (Sainsbury & Urie 2007).

A typical relationship used to determine an initial scale factor is that increasing the zone size requires the critical strain to be reduced proportionally (Wyllie & Mah 2004). Using this relationship a scale factor of approximately 200 was determined for the models presented in this paper. This scaling factor will be examined as part of the following sections.

3.3 Simple geometry stope results

The stopes presented in this section are all rectangular shaped and are 30 m high and 15 m along-strike, and with across-strike widths of 10, 20, 30 and 40 m (Figure 10). All stopes were composed of 0.5 m zones. All stope exposures were across-strike width.

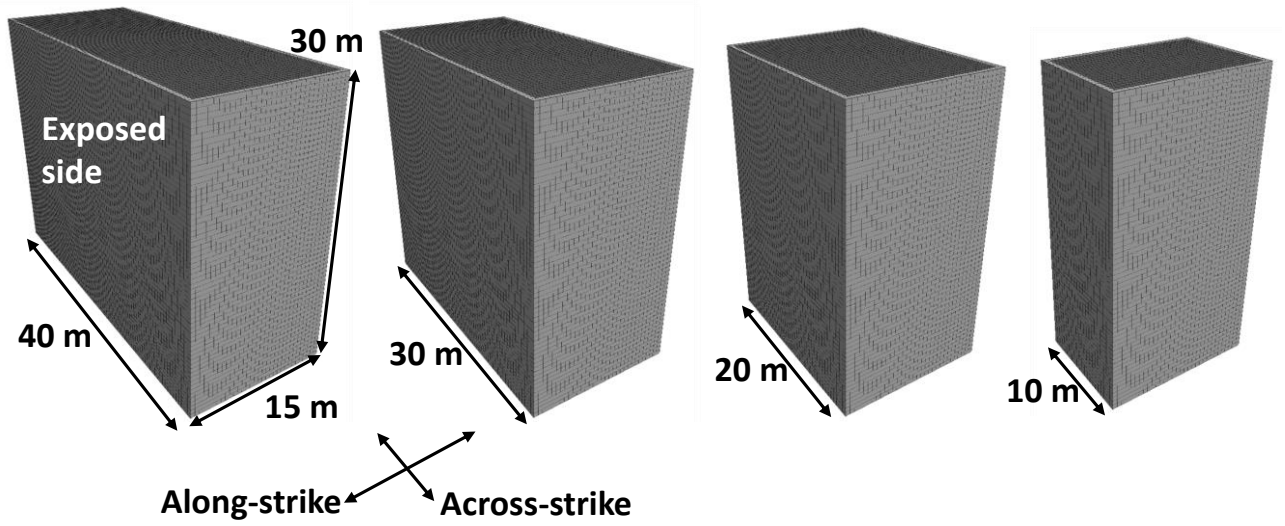

Figure 10 Schematics for simple geometry models

The models were filled with paste using a perfectly plastic model and strain-softening models with critical strain scaling factors of 2, 10, 75, and 200. A series of full-length vertical exposure models were run at various strengths (strengths were varied in 50 kPa increments) and the stability of these exposures were determined. This has been summarised in Figure 11. Some common analytical solution methods are also included on the figure for comparison purposes. The methods included are a 2D wedge, Mitchell's wedge analysis (Kuganatha 2005), and an analysis based on a modification of Terzaghi's (1943) arching theory equation.

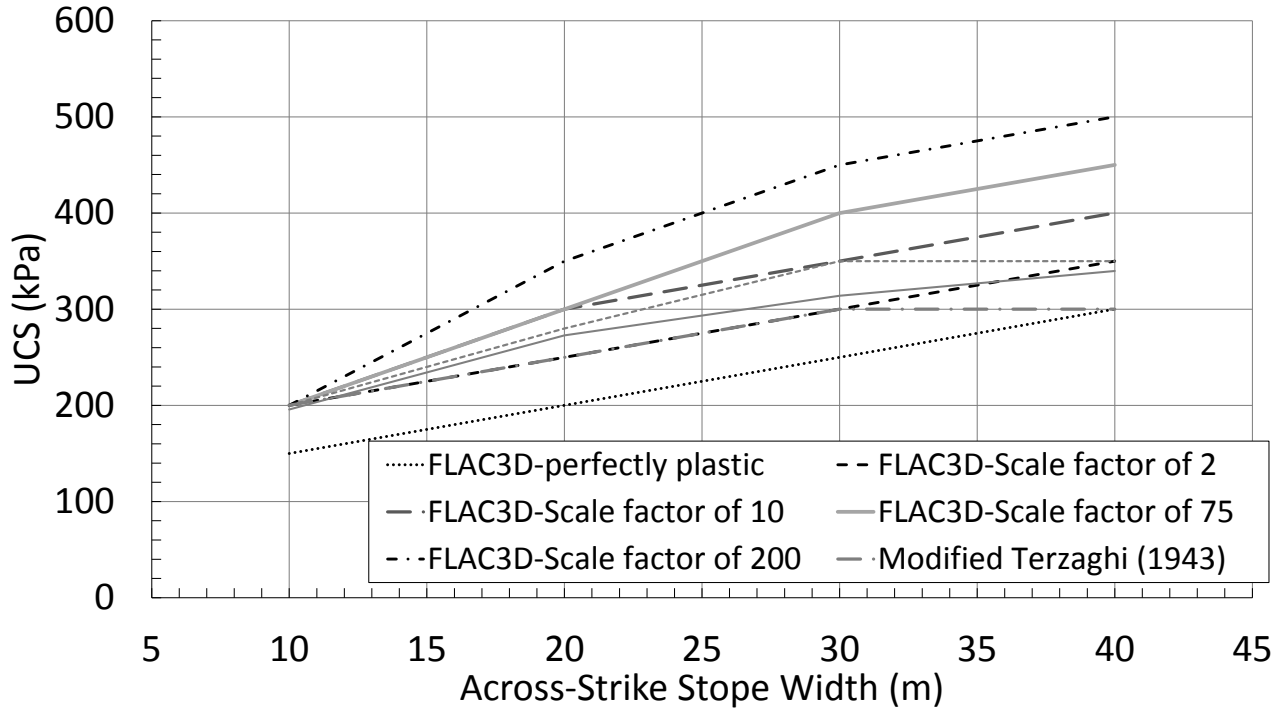

Figure 11 Comparison of various exposure models

This figure shows that the perfectly plastic FLAC3D model required CPB strengths less than the other models. The Mitchell wedge, modified Terzaghi, 2D wedge, and scale factor of 2 model show relatively similar results (within 50 kPa of each other). The scale factor of 200 model required significantly higher CPB strengths to prevent yield. The intermediate scale factors (10 and 75) had exposure strengths between the

other two scale factors. The scale factor of 200 produced results that were unrealistically brittle and the scale factor of 2 produced results which were too ductile. It was decided to proceed with a scale factor of 75 for subsequent modelling, as this was the more conservative option.

All of the simple geometry stopes failed in a similar manner, which is illustrated by the model plots in Figure 12. The stope exposed in this example was a 20 m wide model. Once the CPB is exposed, the fill mass wants to move into the excavation. This movement is resisted at the rock-CPB interface along the edges of the stope. The stress in this area loads up and causes the cohesion in those areas to increase (shown in the first three model plots). Once the maximum cohesive strength of the CPB is reached at the interface, the material fails and the cohesion starts to decrease (model plot 4), indicating an area of shear failure. However, the yielding at the edges means that the toe of the exposure now has to take load. This causes failure in the toe zones (shown in model plots 5 and 6). The two failure areas then start to coalesce into a failure surface. Cross-sections were taken from model plots 5 through to 8 to help show this more clearly.

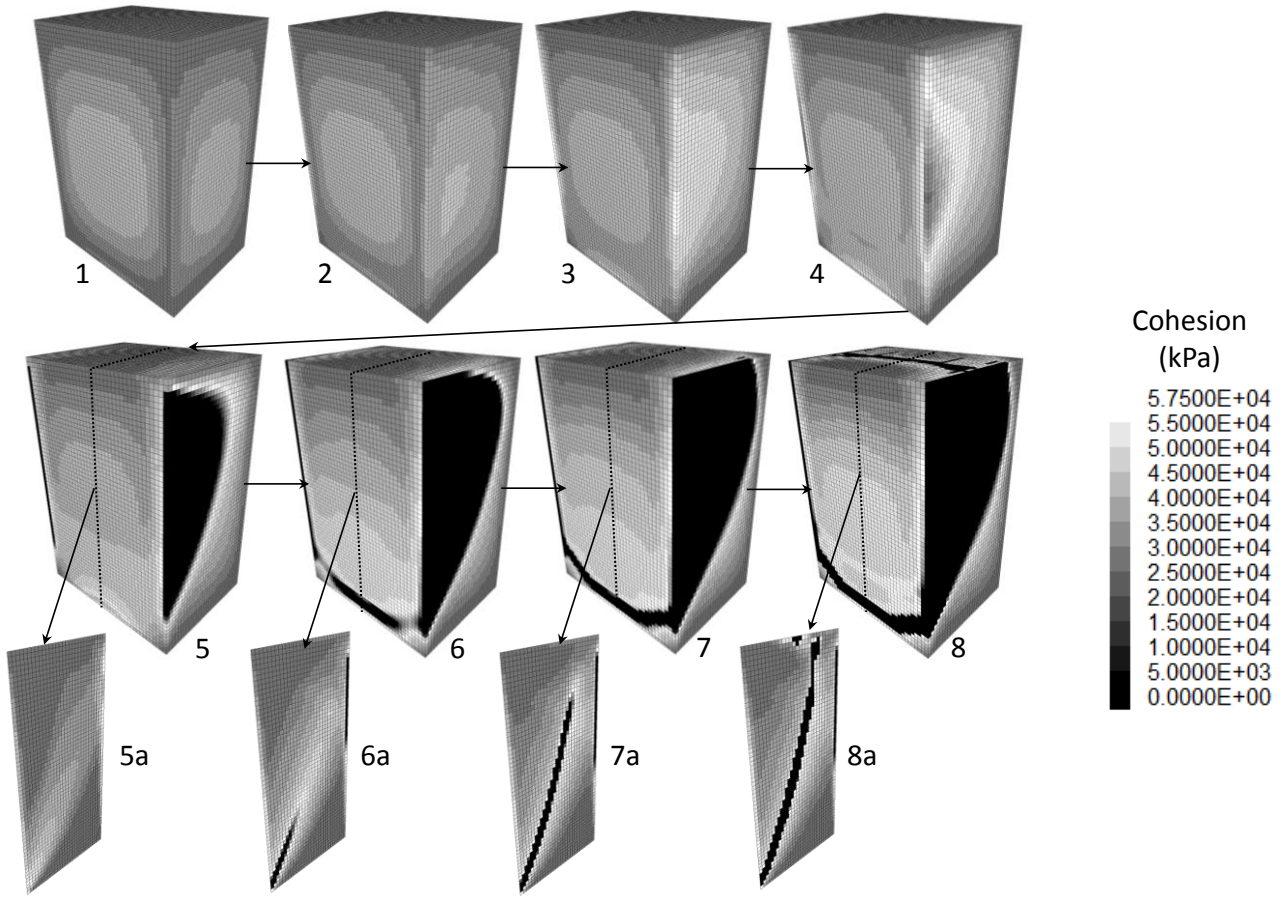

Figure 12 CPB yield in simple geometry model with increased model time-steps

Figure 13 shows the percentage fill dilution from a model study based on a 20 m wide stope using scale factors of 2 and 75. The models were filled with CPB with UCS strengths ranging from 100 to 300 kPa. These stopes were then exposed and their backfill dilution volumes were determined using the methodology presented in Section 3.1. The plot in the figure shows that the amount of backfill dilution decreases with fill strength. This result was expected; however, the shape of the curve was unexpected as a more logarithmic decay relationship was anticipated. The curve indicates that the amount of dilution is very sensitive to relatively small changes in CPB strength. It also contrasts the difference between the brittle and ductile behaviour of the two scaling factors.

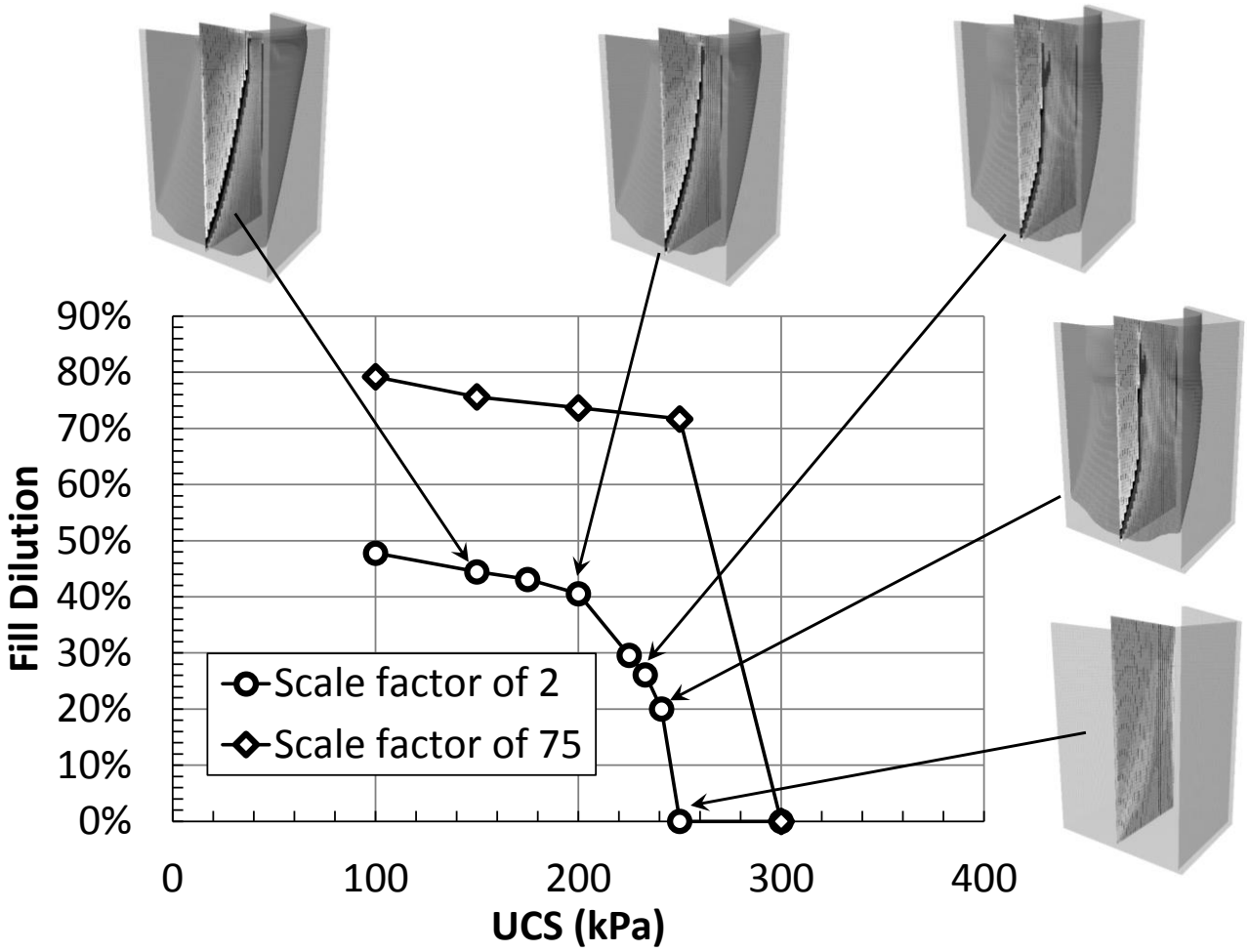

Figure 13 Change in percentage fill dilution due to increasing CPB strength

4 Case study

Figure 14 shows the cavity monitoring surveys from the stopes used in the case study. Figure 14(a) shows an approximate side view of the backfill dilution volume and Figure 14(b) shows the size of the exposure (outlined in black). The stope was approximately 30 m across-strike, 30 m high, and 20 m along-strike.

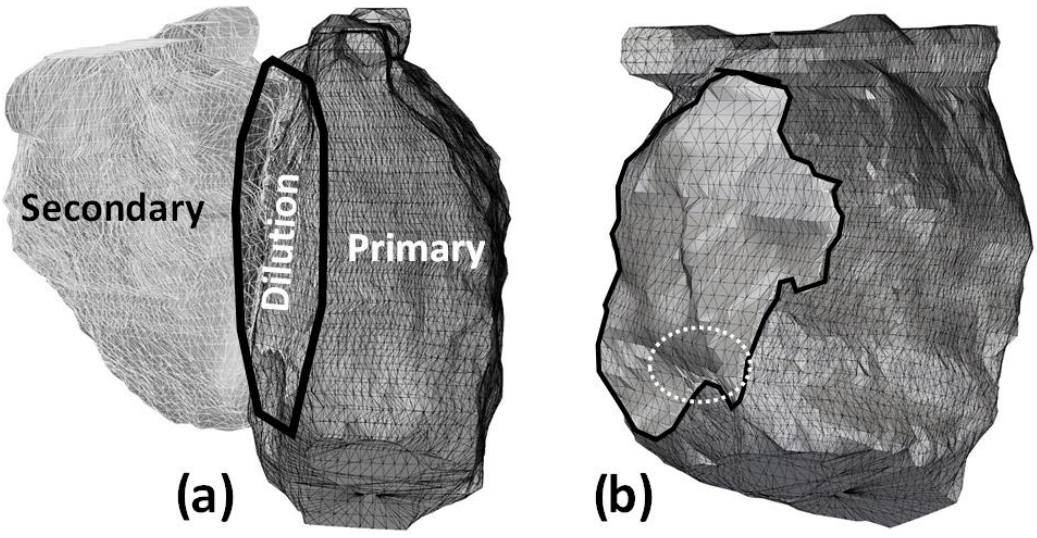

Figure 14 Cavity monitoring survey plots showing backfill dilution from case study stope

The primary stope was mucked and then backfilled. The paste plant quality control (QC) testing indicated that this CPB's strength was 800 kPa after curing for 28 days. However, when the secondary was fired there was approximately 7% backfill dilution from the exposure. This percentage, while not particularly high, was high for the mine in question. The secondary exposure (not analysed in this paper) also produced a similar amount of dilution making the total backfill dilution for the stope approximately 15%. The amount of dilution indicated that there was a discrepancy between the QC and in situ CPB strength.

The stope was filled with different strength CPB ranging from 300 to 800 kPa. These stopes were then exposed by removing the rock mould in the exposure shape shown in Figure 14(b). The stopes were then monitored for failure and, if failure occurred, the amount of dilution was calculated as per the methodology presented in Section 3.1. Figure 15 presents the dilution modelling results.

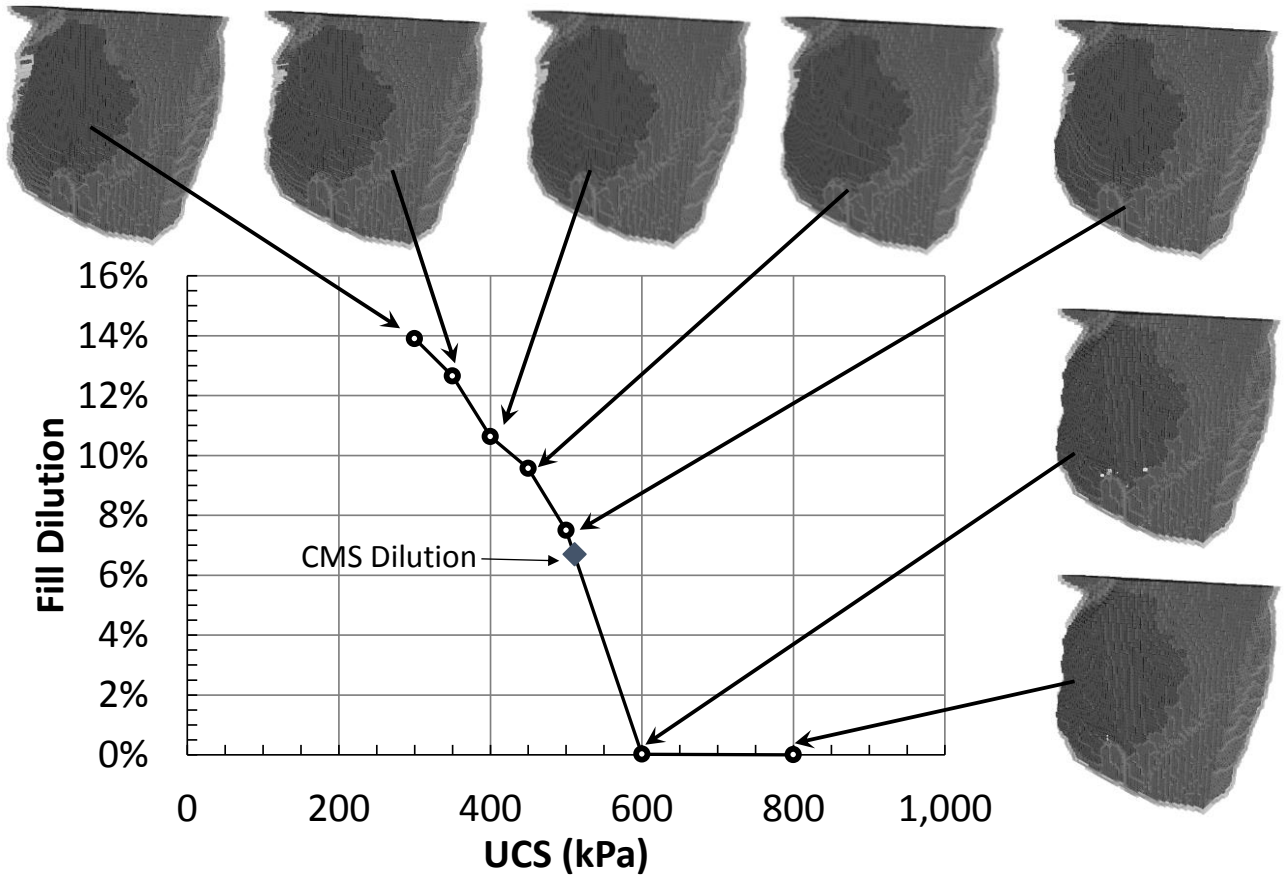

Figure 15 Dilution determined from case study model

This plot indicates that the modelled in situ strength of the CPB is closer to 500 kPa then to 800 kPa as determined by the QC testing. Note that this shape shown in Figure 14(b) is not rectangular. The hydraulic radius of this opening is approximately 5, which corresponds to a rectangular exposure of 15 m wide by 30 m high. Figure 11 suggests the required CPB strength for this stope would be approximately 250 kPa. If one was to assume that the approximate dimensions of the stope are 30 × 30 m, the estimated strength from Figure 11 would be 400 kPa which is closer to the case study's in situ strength. These differences in strength can partially be explained by the overhang of CPB shown in the dashed white circle in Figure 14(b). However, the failure mechanism of the case study stope was different from the one shown in Figure 12.

Figure 16 shows how the CPB yields in the case study stope. The first area of yield is under the overhang identified previously. However, the yielding areas start to ring the exposure with increased time-steps. This progresses until the stable failure surface is reached. At this point, the failure surface forms more of a 'bowl' shape (shown in black on the final cross-section model plot) as opposed to the slide surfaces as observed in Figures 12 and 13.

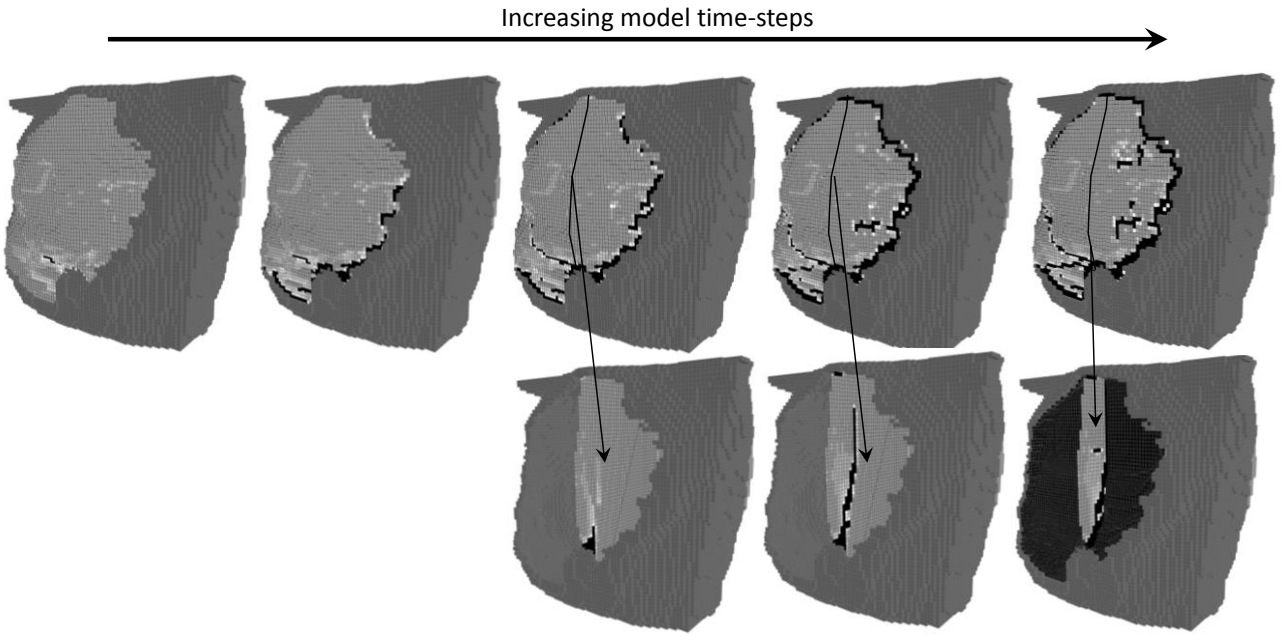

Figure 16 CPB yield in case study model with increased model time-step

This case study has raised two main concerns. The first is that there is a discrepancy between the QC test data and modelling in situ strength suggesting that the stope record should be reviewed to determine any reasons for this discrepancy (assuming these records are available). It also highlights the importance of obtaining in situ CPB samples for comparison to QC testing.

The second is the difference between the case study in situ strength and the strength suggested by Figure 11 for rectangular exposures. The author agrees with Kuganathan (2005) that the analytical methods, like those presented in Figure 11, can be used to estimate backfill strengths, particularly as a starting point. However, the author also recommends that further numerical modelling studies be undertaken if a mine's stope geometry is not the assumed rectangular shape. Part of this exercise needs to include a calibration of these numerical modelling results to the actual performance of the backfill, typically captured in the CMS. The author seconds the recommendation by Fourie and Grice (2015) that ongoing analysis of stope CMS "provides valuable feedback to the performance and quality of the backfill".

5 Conclusion

This paper presents a methodology for estimating the amount of dilution that can be expected given a particular stope geometry filled with CPB of a particular strength. This methodology was examined in a series of simple, rectangular shaped stopes and then in the actual CMS geometry from a test stope.

Three main findings were identified in this paper. The first was the importance of scaling the critical strain to account for a change in model zone size. This was done in the paper by running models at several scaling factors, examining results, and ultimately choosing the realistically conservative factor to finish the modelling. However, it would be useful to develop a more repeatable method for an appropriate scaling factor.

The second is that methodology for estimating fill dilution was used to mimic the CMS from the case study stope. However, more case studies need to be analysed to prove this method. Ideally, the strength of the in situ fill would be known to remove one of the unknowns, highlighting the importance of in situ CPB sampling.

The third was the differences between the results of the analytical and rectangular exposure, and the case study, models. The analytical and rectangular models showed similar trends (depending on the critical strain used). However, the case study model showed different results, both in failure mechanism and

required strength. This suggests that the use of the conventional analytical models for complicated geometry stopes may produce erroneous results.

Acknowledgement

The author acknowledges George Fisher Mine, whose support enabled the writing and presenting of this paper.

References

Fourie, AB & Grice, T 2015, 'Mine backfill', in RJ Jewell & AB Fourie (eds), *Paste and Thickened Tailings – A Guide*, 3rd edn, Australian Centre for Geomechanics, Perth, pp. 245-255.

Hughes, P 2014, 'Underhand cut and fill cemented paste backfill sill beams', PhD thesis, University of British Columbia.

Itasca Consulting Group, Inc. 2015, *FLAC3D: Fast Lagrangian Analysis of Continua in 3 Dimensions, version 5.1,* Itasca Consulting Group, Inc., Minneapolis, MN, http://www.itascacg.com/software/flac3d/new-in-501

Kuganathan, K 2005, 'Geomechanics of mine fill', in Y Potvin, E Thomas & A Fourie (eds), *Handbook on Mine Fill*, Australian Centre for Geomechanics, Perth, pp. 23-47.

Sainsbury, DP & Urie, R 2007, 'Stability analysis of horizontal and vertical paste fill exposures at the Raleigh Mine', *Proceedings of the Ninth International Symposium on Mining with Backfill (Minefill 2007)*, Canadian Institution of Mining, Metallurgy and Petroleum, Westmount, QC, paper no. 2527, 9 p.

Terzaghi, K 1943, *Theoretical Soil Mechanics*, John Wiley & Sons, Inc., New York, NY.

van Gool, B 2007, 'Effects of blasting on the stability of paste fill stopes at Cannington Mine', PhD thesis, James Cook University.

Wyllie, DC & Mah, CH 2005, 'Rock slope engineering', 4th edn, Spon Press, London.